A search for non-collinear ferromagnetism in INVAR

2003 J. Phys.: Condens. Matter 15 521

(http://iopscience.iop.org/0953-8984/15/3/316)

INSTITUTE OF PHYSICS PUBLISHING JOURNAL OF PHYSICS: CONDENSED MATTER

J. Phys.: Condens. Matter **15** (2003) 521–530 PII: S0953-8984(03)53384-7

A search for non-collinear ferromagnetism in INVAR

N Cowlam[1] **and A R Wildes**[2]

[1] Department of Physics and Astronomy, University of Sheffield, Sheffield S3 7RH, UK
[2] Institut Laue-Langevin, BP 156, 38042 Grenoble Cédex 9, France

Received 6 September 2002
Published 13 January 2003
Online at stacks.iop.org/JPhysCM/15/521

Abstract

Measurements have been made to test the proposal that the INVAR effect is associated with a non-collinear ferromagnetic state. Neutron scattering experiments with polarization analysis of the incident and scattered beams have been made to obtain the absolute spin-dependent scattering cross-sections from the archetypal INVAR alloy $Fe_{65}Ni_{35}$. The measured average spin-flip cross-section for this alloy has been found to be close to zero, independent of the scattering vector Q and effectively constant as the sample temperature is reduced from 300 to 4.2 K and the magnetic field increased from 1.4 to 2.0 T. All this suggests that the INVAR sample is a collinear ferromagnet. In addition, the measured spin-flip cross-section is also in poor agreement with calculated curves based on models of the proposed non-collinear state. The magnitudes of the magnetic moments on the iron and nickel atoms in the collinear state have been obtained from the intensities of the Bragg peaks in the non-spin-flip cross-sections. The diffuse scattering between the Bragg peaks has also been analysed to determine the magnetic disorder present. These data have been discussed in the context of different models of the magnetic structure and the results also support the conclusion that $Fe_{65}Ni_{35}$ is a collinear ferromagnet.

1. Introduction

Charles-Edouard Guillaume established that face-centred cubic alloys of iron and nickel with ≈35% nickel exhibit an anomalously small thermal expansion over a wide temperature range (Guillaume 1897). He considered the expansion of these alloys to be 'invariable' and this kind of behaviour has since become known as the INVAR effect. INVAR alloys were historically used in measuring tapes and in the springs of mechanical watches and more recently in the shadow masks in colour television and computer screens. The INVAR effect is clearly related to the ferromagnetism in these alloys, since their coefficient of linear expansion is typically $\alpha = 1.2 \times 10^{-6}$ K^{-1} below the Curie temperature and almost an order of magnitude greater than this in the paramagnetic phase. Macroscopically, the effect can be considered as a massive, spontaneous, volume magnetostriction, in which a magnetostrictive lattice distortion balances the normal thermal expansion of the lattice. It has proved more difficult

to explain the effect satisfactorily on an atomic scale, although it obviously depends on a strong correlation between the value of the magnetic moment and the atomic volume. Weiss, for example, proposed a phenomenological, two-γ-state model for face-centred cubic γ-Fe, in which a high volume ferromagnetic state and a low volume antiferromagnetic state can co-exist (Weiss 1963). The INVAR effect may be explained within this two-γ-state model, if the reduction of the magnetization on raising the temperature is caused by excitation of the low volume antiferromagnetic state, whose presence compensates for the normal thermal expansion. There appears to be little direct experimental evidence (such as line broadening in diffraction experiments) for these two states. However, electronic band theory calculations have predicted a firm correlation between the cell volume and magnetic moment value in γ-Fe (Bagayoko and Callaway 1983) and the existence of two stable states in γ-FeNi alloys (Entel *et al* 1993). Non-collinear ferromagnetism has also been incorporated into electronic band theory calculations of INVAR (Wang *et al* 1997). More recently, a calculation which apparently explained the INVAR effect by making a formal link between the average atomic volume and the magnitude of the non-collinear magnetic order received considerable publicity in *Nature* (van Schilfgaarde *et al* 1999, Mohn 1999).

We have previously used neutron scattering experiments with polarization analysis of both the incident and scattered beams to study non-collinear structures in metallic alloy glasses. We have shown, for example, that non-collinear ferromagnetism exists in $Fe_{83}B_{17}$ glass (Cowley *et al* 1988); that complex magnetic structures are present in the pseudo-binary $(Fe_xNi_{1-x})_{78}B_{12}Si_{10}$ glasses (Cowley *et al* 1991); that substitution of ruthenium in the $Fe_{80-x}Ru_xB_{20}$ glasses suppresses the non-collinear state (Wildes *et al* 1998) and that Fe–Zr glasses with $\approx$10% Zr exhibit a range of non-collinear ferromagnetic structures (Wildes *et al* 2000).

We have therefore undertaken similar experiments on the archetypal INVAR alloy $Fe_{65}Ni_{35}$, specifically to test for the presence of the predicted non-collinear ferromagnetic state. The analysis of the experimental data suggests however that the $Fe_{65}Ni_{35}$ sample is a collinear ferromagnet and this is in agreement with the results of similar neutron scattering studies (Lynn *et al* 1994).

2. Polarized beam neutron scattering

Polarized neutron scattering, in which the four spin-dependent neutron cross-sections are measured, is an ideal technique for studying non-collinear structures in ferromagnets. In one standard configuration (Moon *et al* 1969), the co-ordinate reference for the scattering geometry is defined with y parallel to the scattering vector $Q = 4\pi \sin\theta/\lambda$ and x perpendicular to Q and in the scattering plane. The direction z is perpendicular to the scattering plane and a saturating magnetic field is applied in this direction defining the collinear ferromagnetic axis of the sample. When a neutron passes through the sample with the direction of its spin unchanged, the so-called non-spin-flip scattering cross-sections, $\frac{\partial\sigma^{++}}{\partial\Omega}$ and $\frac{\partial\sigma^{--}}{\partial\Omega}$, can be written

$$\frac{\partial\sigma^{\pm\pm}}{\partial\Omega} = \frac{\partial\sigma_{II}}{\partial\Omega} + \frac{1}{3}\frac{\partial\sigma_{NSI}}{\partial\Omega} + \left|\left\langle \sum_{ij} (b_i \mp d_i S_{zi})(b_j^* \mp d_j^* S_{zj}^*) \exp(\mathrm{i}Q(r_i - r_j)) \right\rangle\right|. \tag{1}$$

Here $\frac{\partial\sigma_{II}}{\partial\Omega}$ and $\frac{\partial\sigma_{NSI}}{\partial\Omega}$ are the isotope incoherent and the nuclear spin incoherent parts of the differential cross-section. The third term includes the coherent scattering (the Bragg peaks), plus the diffuse scattering (equivalent to the Laue monotonic scattering with x-rays) due to presence of two types of atom randomly distributed in the INVAR lattice. In this third term b_i is the nuclear scattering length and the product $d_i S_i$ is the magnetic scattering amplitude, in

which $d_i = \frac{1}{2}\gamma r_0 g_i f_i(Q)$ and $f_i(Q)$ is the magnetic form factor of the ith atom which carries a spin S_i and is situated at the position r_i. These cross-sections clearly contain information about the *collinear* S_z components of the spins.

The corresponding spin-flip cross-sections $\frac{\partial\sigma^{+-}}{\partial\Omega}$ and $\frac{\partial\sigma^{-+}}{\partial\Omega}$ may be written

$$\frac{\partial\sigma^{\pm\mp}}{\partial\Omega} = \frac{2}{3}\frac{\partial\sigma_{NSI}}{\partial\Omega} + \left|\left\langle\sum_{ij}(d_i S_{xi} d_j^* S_{xj}^*)\exp(\mathrm{i}Q(r_i - r_j))\right\rangle\right|. \tag{2}$$

Here the second term now depends on the *non-collinear* S_x components of the spins. If the S_x components are finite, but the directions of the spins are completely random, then the magnetic part of the spin-flip cross-section will follow the square of the form factor $f^2(Q)$ and decrease monotonically with Q.

It is clear from equations (1) and (2) that *the presence of spin-flip* scattering from a ferromagnet indicates that the S_x components of the spins are finite and this *provides unequivocal evidence that the magnetic moments must therefore be non-collinear.*

3. Sample preparation, experimental method and data analysis

An ingot of approximately 20 g was made of the INVAR alloy $Fe_{65}Ni_{35}$ by argon arc melting spectroscopically pure constituents with negligible weight loss. The ingot was cold rolled to 1 mm thick (to improve heat transfer); cut into lengths of approximately 10 cm; annealed under vacuum at 850 °C for 24 h and quenched into iced water to preserve the γ-phase.

The neutron experiments were performed on the IN20 diffractometer at the Institute Laue–Langevin. Polarizing Heusler alloy crystals were used as monochromator and analyser with spin flippers in the incident and scattered beams, to obtain the four spin-dependent cross-sections. Elastic scattering measurements made with an incident wavevector $k = 4.1$ Å^{-1} and horizontal collimators of 60′ gave a wavevector resolution of 2.7×10^{-2} Å^{-1} and an energy resolution of 3 meV at $Q = 3.1$ Å^{-1}. A vertical magnetic field was applied to the sample, using a superconducting cryomagnet to saturate the domains and avoid depolarization effects. Three measurements were made at (1.4 T, 300 K); (2 T, 300 K) and (2 T, 4.2 K), over a range of scattering vectors $1.0 < Q < 6.5$ Å^{-1} and with a data acquisition time of approximately 18 h, because of the low count rates in this type of experiment. Similar scans were made with an indium 'blank' for background subtraction and a standard vanadium sample to obtain the absolute scattering cross-sections. The efficiencies of the polarizing elements were determined by measurements of the flipping ratios from the {111} peak of a standard silicon sample.

The data analysis was performed using our own programs, developed through the studies described above, which are described in Wildes *et al* (1998). The procedures included background subtraction; corrections for absorption and multiple scattering; corrections for incomplete polarization and normalization to the vanadium standard.

An example of the cross-sections obtained is shown in figure 1 from the (2 T, 4.2 K) measurement. The non-spin-flip cross-sections in figure 1(a) contain the first five Bragg peaks of the face-centred cubic γ-FeNi phase (and no others), from whose positions the lattice parameter of the $Fe_{65}Ni_{35}$ alloy was found to be $a = 3.601 \pm 0.005$ Å. An almost identical value was obtained at 300 K. These Bragg peaks are superimposed on a background due to the isotope incoherent and diffuse scattering contributions. The cross-section $\frac{\partial\sigma_{II}}{\partial\Omega} + \frac{1}{3}\frac{\partial\sigma_{NSI}}{\partial\Omega} = 0.166$ barns sr^{-1} atom^{-1} was calculated for this $Fe_{65}Ni_{35}$ alloy using the standard tables (Sears 1992) and this is close to the observed value. The average of the two spin-flip cross-sections (equation (2)) is given in figure 1(b) where the vertical scale is 100 times smaller than in figure 1(a). This average spin-flip cross-section is independent of Q within the error bars.

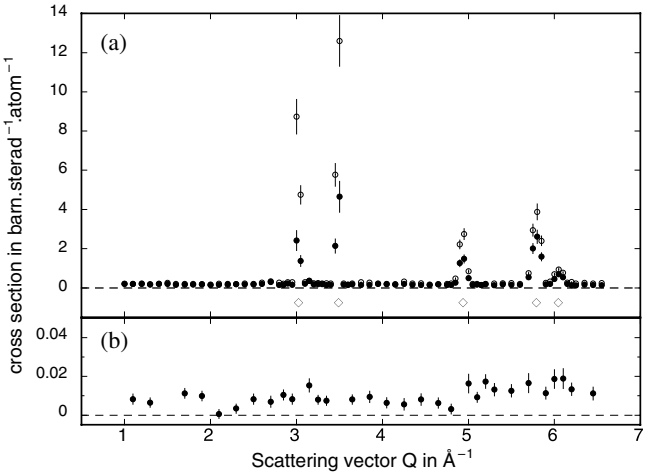

Figure 1. The non-spin-flip (a) and the average spin-flip (b) cross-sections for the INVAR alloy $Fe_{65}Ni_{35}$ are given in absolute units (2 T, 4.2 K data set). The diamonds in (a) mark the positions of the Bragg peaks of the fcc γ-phase. Note the change of scale on the ordinate between (a) and (b).

4. The spin-dependent neutron cross-sections of $Fe_{65}Ni_{35}$

4.1. The average spin-flip cross-sections

Figure 2 shows the average spin-flip cross-sections from the three experiments (1.4 T, 300 K); (2 T, 300 K) and (4.2 T, 4.2 K) plotted on an expanded vertical scale. According to equation (2) the magnitudes of these cross-sections will depend directly on the non-collinear components of the magnetic spins. The nuclear spin incoherent cross-section in equation (2) was calculated from the standard tables (Sears 1992) and found to be extremely small ($\frac{2}{3}\frac{\partial\sigma_{NSI}}{\partial\Omega} = 8.4 \times 10^{-4}$ barns sr^{-1} atom^{-1}). The observed average level of the experimental points is actually larger than this $\approx 7 \times 10^{-3}$ barns sr^{-1} atom^{-1}. It is unlikely that this difference is attributable to a magnetic contribution to the spin-flip cross-sections, since they are independent of Q. This residual level of the cross-section is probably as close to the small, calculated value as the uncertainties in the normalization of the data allow us to reach. To summarize, the average spin-flip cross-sections for the alloy are found to be

(i) close to zero and
(ii) independent (within error bars) of the scattering vector Q.

Furthermore, the three sets of data are identical to within the error bars, implying they are

(i) independent of the sample temperature and
(ii) independent of the applied magnetic field.

Taken together, these observations suggest that the magnetic contribution to the spin-flip cross-sections must be negligible. We are therefore led to conclude that the INVAR alloy is a conventional collinear ferromagnet.

In order to quantify this (null) result further, we have calculated the magnitudes of the spin-flip cross-section expected from non-collinear structures of the type proposed. If there are no spatial correlations between the non-collinear components of the magnetic moments,

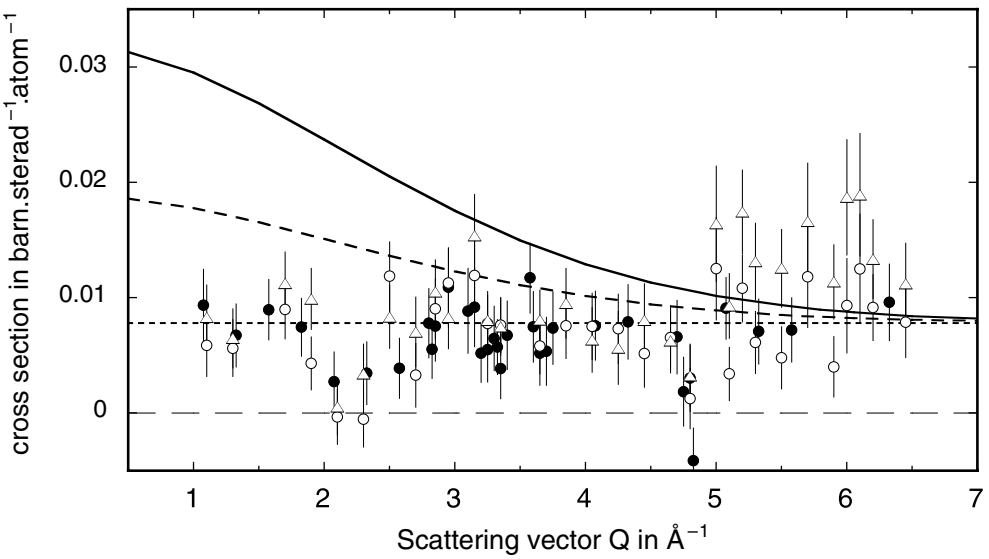

Figure 2. The average spin-flip cross-sections are plotted in absolute units for the three data sets ● = (1.4 T, 300 K); ○ = (2 T, 300 K) and △ = (2 T, 4.2 K). The horizontal dotted line is the effective nuclear spin incoherent scattering cross-section. The dashed curve is the predicted magnetic contribution to the cross-section calculated from equation (3), for the SAJ-RT2 model and the solid curve is the same for the SAJ-RT1 model.

equation (2) becomes

$$\frac{\partial\sigma^{\pm\mp}}{\partial\Omega} = \frac{2}{3}\frac{\partial\sigma_{NSI}}{\partial\Omega} + \frac{d^2}{2}\langle S_x^2\rangle = \frac{2}{3}\frac{\partial\sigma_{NSI}}{\partial\Omega} + \frac{d^2}{2}[S^2 - \langle S_z^2\rangle] \tag{3}$$

which can be calculated when the $\langle S_x^2\rangle$ or $\langle S_z^2\rangle$ values are known.

The two models intended to imitate the non-collinear structures predicted to exist in INVAR have been derived from the figures given in van Schilfgaarde *et al* (1999). Their figure 3 (the volume dependence of the magnetic moment) shows that the value of average moment $\langle\mu\rangle = 1.29\ \mu_B$ we have used for INVAR at 300 K corresponds to an atomic volume $72 < \Omega < 74$ au. The individual moments are then $\mu_{\mathrm{Fe}} \approx 2.1\ \mu_B$ and $\mu_{\mathrm{Ni}} \approx 0.57\ \mu_B$. Their figure 2 (for the spin–spin correlation functions) then shows that at this value of atomic volume Ω, the moments on the nearest neighbour iron atoms are randomly aligned and the next nearest neighbour moments are collinear. About one-half of the moments on the nearest neighbour nickel atoms are collinear and the rest canted at angles ≈40° to the collinear direction. There are 12 first and six second nearest neighbours in the fcc lattice and for a random substitutional alloy the probability of finding an atom on a given site depends only on the concentration. This means an average occupation of ⟨8Fe/4Ni⟩ and ⟨4Fe/2Ni⟩ in the first two neighbour shells. We have interpreted the random alignment of the nearest neighbour magnetic moments in this (SAJ-RT1) model to mean simply that one-third of them point 'upwards'; one-third 'horizontally' and the remainder 'downwards'. The second model (SAJ-RT2) was obtained by a simple visual inspection of the four schematic diagrams of the magnetic structures in figure 1 of van Schilfgaarde *et al* (1999). At an atomic volume of $\Omega = 73.7$ au, within the range considered above, the figure shows that about one-third of the iron moments are aligned along the direction of net magnetization, one-third at roughly 15° from this direction and the remaining one-third at about 30° from it. About half of the magnetic moments on the nickel

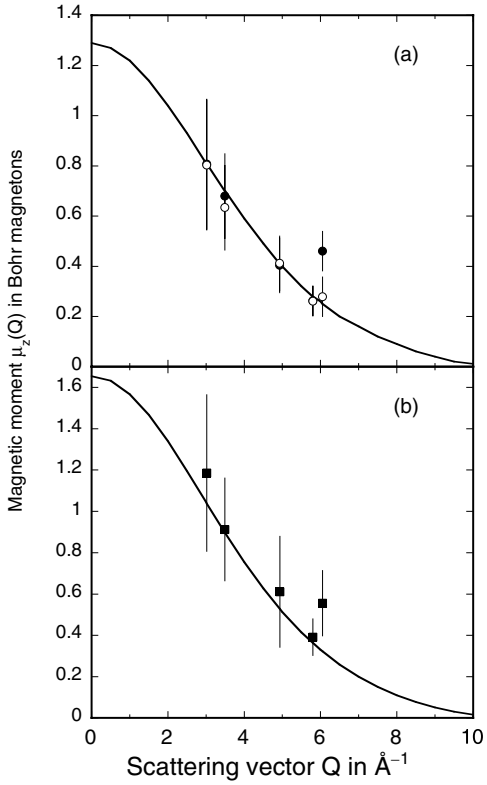

Figure 3. The data points in (a) and (b) show the collinear component of the average magnetic moment per site $\mu_z f(Q)$ derived from the intensities of the Bragg peaks in the non-spin-flip cross-sections, compared with the prediction of the EM model, using equation (6). (a) ● = (1.4 T, 300 K) ○ = (2 T, 300 K)—note that some of the data points are superimposed. (b) ■ = (2 T, 4.2 K).

atoms appear to be aligned along the direction of net magnetization and the remainder are about 10° from it.

The magnetic moments and their dS_z components for these two (SAJ-RT1 and SAJ-RT2) models are given in table 1, from which the corresponding cross-sections were calculated using equation (3). The horizontal dotted curve in figure 2 is drawn at the 'background' level of 7×10^{-3} barns sr^{-1} atom^{-1} and represents the isotropic incoherent scattering, while the dashed curve represents the magnetic contribution for the SAJ-RT2 model. The solid curve is that for the SAJ-RT1 model, where the magnetic contribution is larger because of the random directions of the magnetic moments on the iron atoms. The Q dependence of the calculated cross-sections of both these models is obviously incompatible with the experimental data and reinforces the conclusions that INVAR is a collinear ferromagnet on the basis of this experimental evidence.

4.2. The non-spin-flip cross-sections

The analysis in the section above points to the presence of collinear ferromagnetism in the INVAR alloy and equation (1) shows that the non-spin-flip cross-sections will contain information about the collinear components of the magnetic spins. The magnitudes of the non-spin-flip cross-sections $\frac{\partial\sigma^{++}}{\partial\Omega}$ and $\frac{\partial\sigma^{--}}{\partial\Omega}$, are different at the same Bragg peak depending on

Table 1. The values of the magnetic moments and spin components are given for two non-collinear structures of $Fe_{65}Ni_{35}$ INVAR at 300 K, which have been used to calculate the cross-sections shown in figures 2 and 5.

	Temperature 300 K		
	$\mu_{Fe} = 2.1\ \mu_B$	$\mu_{Ni} = 0.57\ \mu_B$	
Model	Atom	Percentage of total	Collinear component
SAJ-RT1	Fe	55	S_z
	Fe	22	0
	Fe	22	$-S_z$
	Ni	67	S_z
	Ni	33	$S_z \cos 40°$
SAJ-RT2	Fe	33	S_z
	Fe	33	$S_z \cos 15°$
	Fe	33	$S_z \cos 30°$
	Ni	50	S_z
	Ni	50	$S_z \cos 10°$

the sign inside the third term of equation (1). The average magnetic scattering amplitude $\langle \mathrm{d}S_z \rangle$ per atom can be obtained in absolute units, from the ratio R of the magnitudes of each of the five Bragg peaks,

$$R = \frac{\partial\sigma^{--}}{\partial\Omega} \Big/ \frac{\partial\sigma^{++}}{\partial\Omega} = \left\langle \frac{b + \mathrm{d}S_z}{b - \mathrm{d}S_z} \right\rangle^2, \tag{4}$$

and from this the collinear component of the mean magnetic moment per atom (μ_z in Bohr magnetons) can be derived,

$$\langle \mathrm{d}S_z \rangle = \tfrac{1}{2}\gamma r_0 \langle g S_z f(Q) \rangle = 0.2695 \times 10^{12} \langle \mu_z f(Q) \rangle \text{ cm}. \tag{5}$$

In fact, it is convenient to compare the experimental values of $\mu_z f(Q)$ with those calculated for various models of the magnetic structures, over the measured Q range,

$$\mu_z f(Q) = 0.65\mu_{Fe} f_{Fe}(Q) + 0.35\mu_{Ni} f_{Ni}(Q). \tag{6}$$

This can be done using the tabulated five-parameter fits to the magnetic form factors (Brown 1995).

In the simplest model of INVAR, the iron and nickel atoms can be considered to have the same values of saturation magnetic moment as in their elemental metals, $\mu_{Fe} = 2.22\ \mu_B$ and $\mu_{Ni} = 0.606\,\mu_B$ and this will be referred to as the EM model. The average magnetic moment of the $Fe_{65}Ni_{35}$ alloy is then $\mu_z = 1.66\,\mu_B$ at 4.2 K, close to the value ($1.58\ \mu_B$) obtained from bulk magnetic measurements (Crangle and Hallam 1963, Wassermann 1990). The corresponding values at room temperature $\mu_{Fe} = 1.73\ \mu_B$ and $\mu_{Ni} = 0.47\ \mu_B$ can be obtained by scaling the saturation values, using the spontaneous magnetization curves $M(T)/M_0$ (Yamada *et al* 1982, Yamada and du Trémolet de Lachessserie 1984).

Only poor agreement was obtained between experiment and calculation when the $f^+_{Fe}(Q)$ and $f^+_{Ni}(Q)$ form factors expected for an itinerant ferromagnet were used in equation (6). The $f^+_{Fe}(Q)$ form factor falls more rapidly with Q than $f^+_{Ni}(Q)$ and so the $f^{3+}_{Fe}(Q)$ form factor was substituted. The results of this calculations are shown in figures 3(a) (1.4 T, 300 K, 2 T, 300 K) and (b) (2 T, 4.2 K) and the level of agreement with the data is quite satisfactory. Note that apart from the substitution of the $f^{3+}_{Fe}(Q)$ form factor for the $f^+_{Fe}(Q)$ there are no adjustable parameters between the calculated lines and the data points in figure 3.

Table 2. The values of the magnetic moments are given for three collinear structures of $Fe_{65}Ni_{35}$ INVAR. The EM model has been used with the tabulated magnetic form factors, to calculate the continuous curves in figures 3(a) and (b) and the EM-4K model used to calculate the cross-sections shown in figure 4.

		Magnetic moment value in μ_B		
Model	Temperature (K)	Fe	Ni	⟨mean⟩
EM	4.2	2.22	0.61	1.66
	300	1.73	0.47	1.29
D3	4.2 (estim)	3.20	1.20	2.50
	300	2.02	1.37	1.79
SAJ-4K	4.2	2.45	0.63	1.81

Two other possible models of the magnetic structure of INVAR were also examined. One was based on the recent polarized neutron diffraction measurements (Brown *et al* 2000, 2001) made on single crystals of $Fe_{65}Ni_{35}$ using the D3 diffractometer at the ILL. The magnetic moment values obtained in this work are rather large and the ratio of their values $\mu_{Fe}/\mu_{Ni} \approx 1.5$ is quite different from that for the EM model $\mu_{Fe}/\mu_{Ni} \approx 3.7$—see table 2. The calculated curve for this (D3 model) was in poor agreement with the data points, particularly with the (2 T, 4.2 K) data. The other model was based on the prediction (van Schilfgaarde *et al* 1999, their figure 3(a)) that the magnetic moment values are slightly *greater* than the elemental ones at the largest values of atomic volume. These larger moment values (SAJ-4K model of table 2) led to reasonable agreement with the (2 T, 4.2 K) data of figure 3(b), but a less satisfactory description of the diffuse scattering which will be discussed below.

4.3. The diffuse component of the non-spin-flip cross-sections

The magnitude of the non-spin-flip cross-sections between the Bragg peaks is obtained from equation (1),

$$\frac{\partial\sigma^{\pm\pm}}{\partial\Omega} = \frac{\partial\sigma_{II}}{\partial\Omega} + \frac{1}{3}\frac{\partial\sigma_{NSI}}{\partial\Omega} + \frac{\partial\sigma_{Diff}}{\partial\Omega} \tag{7}$$

where the third term arises from the presence of the two types of atom (each with its own value of magnetic moment) randomly distributed in the lattice,

$$\frac{\partial\sigma^{\pm\pm}_{Diff}}{\partial\Omega} = \langle(b \mp \mathrm{d}S_z)^2\rangle - \langle(b \mp \mathrm{d}S_z)\rangle^2. \tag{8}$$

The cross-sections in equation (7) were calculated for all the models described above together with the tabulated data for the incoherent cross sections. Figure 4 shows the result for the EM model at 4.2 K, superimposed on the measured (2 T, 4.2 K) data plotted on an extended vertical scale. The data points of the two cross-sections overlap within the error bars and the calculated cross-sections follow the trend of the data points. This simple EM model therefore provides a satisfactory description of the data at 4.2 K. The average spin-flip cross-section is also shown on the same scale In all these models INVAR is accepted to be a collinear ferromagnet at 4.2 K, so this spin-flip cross-section is just from the nuclear spin incoherent scattering which is independent of Q. Figure 5 shows the calculated cross-sections for the EM model at room temperature 300 K, superimposed on the (2 T, 300 K) data. The agreement is again quite satisfactory. The non-spin-flip cross-sections were also calculated for the two non-collinear models (SAJ-RT1 and SAJ-RT2) and the two dotted curves in figure 5 are for the SAJ-RT1

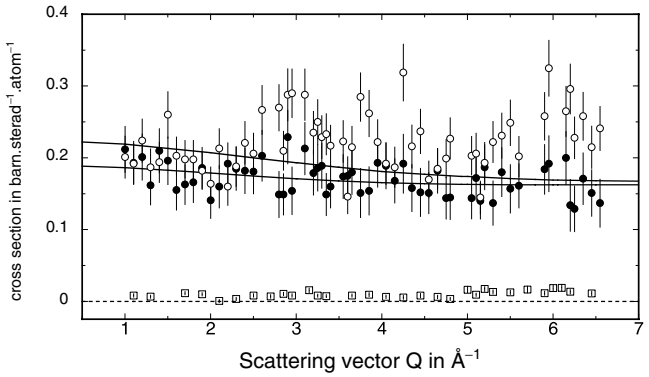

Figure 4. The non-spin-flip cross-sections between the Bragg peaks are plotted in absolute units on an expanded scale for the (2 T, 4.2 K) data set. The continuous lines represent the $\frac{\partial\sigma^{++}}{\partial\Omega}$ and $\frac{\partial\sigma^{--}}{\partial\Omega}$ cross-sections calculated using equations (7) and (8), with the parameters for the EM model. The lower data set is the spin-flip cross-section, on the same scale.

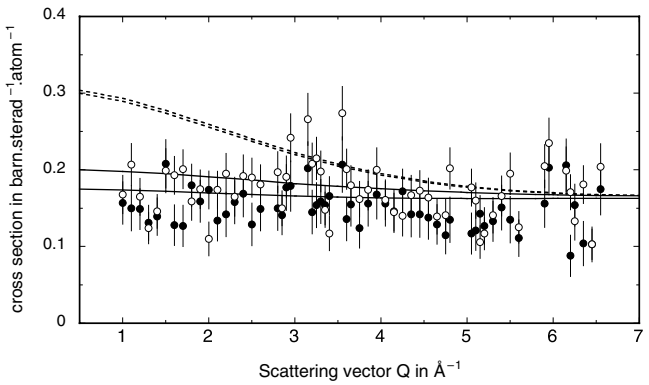

Figure 5. The non-spin-flip cross-sections for the (2 T, 300 K) data set are shown for comparison with figure 4. The continuous curves are the cross-sections calculated for the EM-RT model and the dotted curves for the SAJ-RT1 model.

model that has the greatest degree of magnetic disorder. The exaggerated Q dependence of these cross-sections does not provide a good fit to the data points.

5. Discussion and conclusions

The spin-dependent scattering cross-sections of the INVAR alloy $Fe_{65}Ni_{35}$ have been obtained by polarized beam neutron scattering measurements, to test for the presence of a non-collinear ferromagnetic state.

The principal finding is that the average spin-flip cross-sections for this alloy are close to zero. All three data sets (1.4 T, 300 K), (2 T, 300 K) and (2 T, 4.2 K) can be superimposed within their error bars, indicating that they are independent of temperature and applied magnetic field. Their sum is independent of the scattering vector Q and completely lacks the form-factor dependence of the cross-sections predicted for the model non-collinear ferromagnetic structures examined. Taken together these observations imply that the $Fe_{65}Ni_{35}$ INVAR alloy sample is likely to be a conventional collinear ferromagnet. This conclusion is also supported

by the inelastic polarized neutron beam measurements of Lynn *et al* (1994), which are closely related to our present work.

In addition, the intensities of the Bragg peaks in the non-spin-flip cross-sections have been measured to obtain the values of the (collinear components) of the magnetic moments on the iron and nickel atoms. Good agreement is obtained with the experimental data using a simple model based on a collinear structure in which the iron and nickel atoms have magnetic moment values similar to the ones in their elemental metals. The magnitudes of the non-spin-flip cross-sections between the Bragg peaks have also been examined. They have been shown to be consistent with the sum of the nuclear incoherent scattering and the diffuse scattering contributions due to the presence of the two types of atom, with their two different values of magnetic moment in the INVAR lattice.

Acknowledgments

The authors would like to thank the Institut Laue–Langevin for the use of the IN20 instrument, Professor P J Brown for helpful discussions and Mr J Newell for his assistance in the sample preparation.

References

Bagayoko D and Callaway J 1983 *Phys. Rev.* B **28** 5419–22
Brown P J 1995 *International Tables for Crystallography* vol C, ed A J C Wilson (Dordrecht: Kluwer) pp 391–9
Brown P J, Neumann K-U and Ziebeck K R A 2000 *Institut Laue–Langevin Annual Report* pp 14–15
Brown P J, Neumann K-U and Ziebeck K R A 2001 *J. Phys.: Condens. Matter* **13** 1563–9
Cowley R A, Cowlam N and Cussen L D 1988 *J. Physique Coll.* **49** C8 1285–6
Cowley R A, Patterson C, Cowlam N, Ivison P K, Martinez J and Cussen L D 1991 *J. Phys.: Condens. Matter* **3** 9521–37
Crangle J and Hallam G C 1963 *Proc. R. Soc.* A **272** 119
Entel P, Hoffmann E, Mohn P, Schwartz K and Moruzzi V L 1993 *Phys. Rev.* B **47** 8706–10
Guillaume C E 1897 *C. R. Acad. Sci., Paris* **125** 235–8
Lynn J W, Rosov N, Acet M and Bach H 1994 *J. Appl. Phys.* **75** 6069–71
Mohn P 1999 *Nature* **400** 18–19
Moon R M, Riste T and Koehler W C 1969 *Phys. Rev.* **181** 920–31
Sears V F 1992 *Neutron News* **3** 26–37
van Schilfgaarde M, Abrikosov I A and Johansson B 1999 *Nature* **400** 46–9
Wang Y, Stocks G M, Nicholson D M C, Sheldon W A, Antropov V P and Harmon B N 1997 *J. Appl. Phys.* **81** 3873–5
Wassermann E F 1990 *Ferromagnetic Materials* vol 5, ed K H J Buschow and E P Wohlfarth (Amsterdam: Elsevier) pp 237–322
Weiss R J 1963 *Proc. R. Soc.* A **82** 281–2
Wildes A R, Cowlam N, Al-Heniti S, Kiss L F and Kémeny T 2000 *Physica* B **276–278** 712
Wildes A R, Cowley R A, Al-Heniti S, Cowlam N, Kulda J and Lelièvre-Berna E 1998 *J. Phys.: Condens. Matter* **10** 2617–30
Yamada O and du Trémolet de Lachesserie F 1984 *J. Phys. Soc. Japan* **53** 729
Yamada O, Ono F, Nakai I, Maruyama H, Arae F and Ohta K 1982 *Solid State Commun.* **42** 473